

Sex-dependent expression of Oat3 (Slc22a8) and Oat1 (Slc22a6) proteins in murine kidneys

Davorka Breljak, Hrvoje Brzica, Douglas H. Sweet, Naohiko Anzai and Ivan Sabolic
Am J Physiol Renal Physiol 304:F1114-F1126, 2013. First published 6 February 2013;
doi: 10.1152/ajprenal.00201.2012

You might find this additional info useful...

This article cites 41 articles, 27 of which you can access for free at:
<http://ajprenal.physiology.org/content/304/8/F1114.full#ref-list-1>

Updated information and services including high resolution figures, can be found at:
<http://ajprenal.physiology.org/content/304/8/F1114.full>

Additional material and information about *American Journal of Physiology - Renal Physiology* can be found at:
<http://www.the-aps.org/publications/ajprenal>

This information is current as of April 21, 2013.

American Journal of Physiology - Renal Physiology publishes original manuscripts on a broad range of subjects relating to the kidney, urinary tract, and their respective cells and vasculature, as well as to the control of body fluid volume and composition. It is published 24 times a year (twice monthly) by the American Physiological Society, 9650 Rockville Pike, Bethesda MD 20814-3991. Copyright © 2013 the American Physiological Society. ISSN: 1522-1466. Visit our website at <http://www.the-aps.org/>.

Sex-dependent expression of Oat3 (Slc22a8) and Oat1 (Slc22a6) proteins in murine kidneys

Davorka Breljak,¹ Hrvoje Brzica,¹ Douglas H. Sweet,² Naohiko Anzai,³ and Ivan Sabolic¹

¹Molecular Toxicology, Institute for Medical Research and Occupational Health, Zagreb, Croatia, ²Department of Pharmaceutics, Virginia Commonwealth University, Richmond, Virginia; and ³Department of Pharmacology and Toxicology, Dokkyo Medical University School of Medicine, Tochigi, Japan

Submitted 5 April 2012; accepted in final form 5 February 2013

Breljak D, Brzica H, Sweet DH, Anzai N, Sabolic I. Sex-dependent expression of Oat3 (Slc22a8) and Oat1 (Slc22a6) proteins in murine kidneys. *Am J Physiol Renal Physiol* 304: F1114–F1126, 2013. First published February 6, 2013; doi:10.1152/ajprenal.00201.2012.—In the mouse kidney, organic anion transporter 3 (mOat3, Slc22a8) was previously localized to the basolateral membrane (BLM) of proximal tubule (PT), thick ascending limb of Henle, macula densa, distal tubule, and cortical collecting duct. However, the specificity of anti-Oat3 antibodies (Oat3-Ab) used in these studies was not properly verified. Moreover, the sex-dependent expression of mOat3, and of the functionally similar transporter mOat1 (Slc22a6), in the mouse kidney has been studied at mRNA level, whereas their protein expression is poorly documented. Here we investigated 1) specificity of Oat3-Abs by using *Oat3* knockout (KO) mice, 2) cell localization of renal mOat3 with a specific mOat3-Ab, 3) sex-dependent expression of renal mOat3 and mOat1 proteins, and 4) hormone(s) responsible for observed sex differences. As previously shown, an Oat3-Ab against the rat protein stained the BLM of various nephron segments in wild-type (WT) mice, but the same staining pattern was noted along the nephron of *Oat3* KO mice. However, the mOat3-Ab exclusively stained the BLM of PT in WT mice, where it colocalized with the mOat1 protein, whereas no staining of Oat3 protein was noted in the kidney of *Oat3* KO mice. The expression of mOat3 protein was lower in male mice, upregulated by castration, and downregulated by testosterone treatment. The expression of mOat1 protein was stronger in males, downregulated by castration, and upregulated by testosterone treatment. Thus, at the protein level, mOat3 and mOat1 exhibit sex-dependent expression with an opposite pattern; mOat3 is female dominant due to androgen inhibition, while mOat1 is male dominant due to androgen stimulation.

gender differences; immunocytochemistry; mouse nephron; organic anion transporters; proximal tubule; sex differences; sexual dimorphism; *Oat3* knockout

IN THE MAMMALIAN KIDNEY, various endogenous and exogenous organic anions (OA), such as anionic metabolites, therapeutic drugs, and environmental toxins, are eliminated by several OA transporters that operate as exchangers and belong to the large family of solute carriers 22 (OAT/SLC22 in humans; Oat/Slc22 in animals). In proximal tubule epithelial cells, transport of OA from blood to urine is mediated by two distinct types of OATs/Oats; those localized in the basolateral membrane (BLM) mediate the cellular uptake of OA from blood, whereas those localized in the brush border membrane (BBM) mediate the exit of OA into the tubular lumen. In humans and rodents (such as mice and rats), two major BLM transporters responsible for the first step in the renal elimination of a broad range

of OA are OAT1/Oat1 (SLC22A6/Slc22a6) and OAT3/Oat3 (SLC22A8/Slc22a8; Refs. 1, 10, 30, 33, 40).

In this study we will focus on the murine orthologs of these OATs, e.g., mouse Oat3 (mOat3) and mouse Oat1 (mOat1). When originally isolated from the mouse kidney, the functional activity of each transporter was unknown, and mOat1 was initially named the novel kidney transporter (NKT; Ref. 25), whereas mOat3 was identified as the reduced in osteosclerosis transporter (Roct; Ref. 4). Subsequently, NKT and Roct were characterized as Oats and members of the Slc22 family. It is assumed that both transporters have 12 putative transmembrane domains with NH₂ and COOH termini located intracellularly, several putative *N*-linked glycosylation sites on the large first extracellular loop, and several potential phosphorylation sites in the third intracellular loop (10, 30, 34, 40). Knockout (KO) mouse models for *Oat3* (*Oat3* KO, *Oat3*^{-/-}) and *Oat1* (*Oat1* KO, *Oat1*^{-/-}) have been generated to elucidate the functional role of mOat1 and mOat3 in renal secretion of various endogenous metabolites, xenobiotics, and drugs from the body (14, 36, 38, 39).

Northern blot and RT-PCR studies indicated that the expression of mRNAs for *mOat1* and *mOat3* is mainly restricted to the kidney and brain and largely negative in most other extrarenal tissues (33, 34). Northern blotting revealed that *mOat1* mRNA is expressed abundantly in kidney, weakly in brain, and not at all in heart, placenta, lung, liver, spleen, and stomach (14, 23). Similar tissue distribution was shown for *mOat3* mRNA, which is highly expressed in kidney, weakly in brain and eyes, and not detected in liver, heart, spleen, lung, skeletal muscle, testis, and pancreas (4, 21, 29, 36). The RT-PCR studies detected *mOat3* mRNA in the choroid plexus and capillary endothelial cells of the mouse brain (29, 36).

The mOat1 and mOat3 proteins have been localized in the mouse kidney and brain in several immunocytochemical studies. In the kidney, the mOat1 protein was detected in the BLM of proximal convoluted tubules (PCT; mainly S2 segment), whereas the initial S1 segment was Oat1 negative (18) or weakly positive (2). Other parts of the mouse nephron were Oat1 negative (2, 14, 18). The specificity of anti-Oat1 antibody and the exact cell localization of mOat1 in kidney were previously verified in the *Oat1* KO mouse model (14). In contrast, the renal mOat3 protein was localized to the BLM in proximal tubules and other parts of the mouse nephron including thick ascending limb of Henle (TALH), distal tubule (DT), connecting tubule, and cortical collecting duct (CCD; Refs. 2, 28). Conflicting data concerning the immunolocalization of mOat3 protein in macula densa (MD) cells in the mouse kidney have been reported; in two studies, the mOat3 protein was detected at the basolateral side of MD cells (2, 28), whereas in

Address for reprint requests and other correspondence: D. Breljak, Molecular Toxicology, Institute for Medical Research and Occupational Health, Ksaverska cesta 2, HR-10000 Zagreb, Croatia (e-mail: dbreljak@imi.hr).

the study by Hwang et al. (18), the MD cells were mOat3 negative. However, the specificity of anti-Oat3 antibodies used in these studies with mouse organs was not properly verified (e.g., in the *Oat3* KO mouse model). Therefore, the exact localization of Oat3 protein in the mouse kidney is still controversial.

In rodents, the sex-dependent expression of various Oats in liver and kidneys, which is generated by stimulatory or inhibitory actions of sex hormones after puberty, has been described in numerous publications (5, 7, 8, 9, 20, 23, 24, 31, 32, 39). In the mouse kidney, the sex-dependent expression of *mOat1* and *mOat3* mRNAs has been reported. By using branched DNA signal amplification and real time RT-PCR analysis, three independent groups reported that the expression of renal *mOat1* mRNA is significantly higher in male than in female mice (9, 15, 39). However, the relative expression of renal *mOat3* mRNA was different from that of *mOat1* mRNA, e.g., it was higher in females than in males in J129 strain, whereas in C57Bl/6 strain of mice, it was sex independent in one study (9) and female dominant in another study (39). Recently, it was shown that the staining intensity of mOat1 in the proximal tubule of adult mice is higher in males than in females (18). Thus, while the sex-dependent expression of renal mOat1 and mOat3 has been well investigated at the mRNA level, the sex-dependent expression of these transporters at the protein level has been poorly documented.

The purpose of this study was to 1) verify specificity of the anti-Oat3 antibodies by using an *Oat3* KO mouse model, 2) reinvestigate the renal localization of mOat3, 3) investigate the sex-dependent expression of mOat3 and mOat1 proteins in the kidney of adult mice, and 4) define which hormone(s) are responsible for these sex differences.

MATERIALS AND METHODS

Animals and treatment. Adult (age 2–3.5 mo) male and female mice of C57Bl/6 strain from the breeding colony at the Rudjer Boskovic Institute in Zagreb, Croatia, were used. Male mice were castrated by scrotal route at an age of 2 mo. The sham-operated males underwent the same procedure, except that the testes were not removed. The operations were performed while the animals were under chloral hydrate-induced anesthesia (0.36 g/kg body mass, 3 μ l/g body mass ip). One month later, castrated and sham-operated animals were used in experiments. Some of the castrated male mice (3 animals in each group) underwent treatment with either testosterone enanthate (Galenika, Beograd, Serbia) or estradiol dipropionate (Sigma-Aldrich, St. Louis, MO) (each 2.5 mg·kg body mass⁻¹·day⁻¹ sc for 14 days; hormones were dissolved in sunflower oil). The castrated control mice

(3 animals in group) were treated with an equivalent amount of the sunflower oil (2.5 ml·kg body mass⁻¹·day⁻¹ sc for 14 days). The wild-type (WT) and *Oat3* KO (*Oat3*^{-/-}) male and female adult mice (strain C57Bl/6) were raised in the animal facility of Virginia Commonwealth University, Division of Animal Resources, and described previously (36). Before and during experiments, mice were housed under a 12-h light-dark cycle and had ad libitum access to standard pellet food and water. The studies were approved by the Ethics Committee of the Institute in Zagreb.

Chemicals and antibodies. Various chemicals and reagents were of analytical or molecular biology grade, and their commercial source was either from Kemika (Zagreb, Croatia), Sigma-Aldrich, or Fisher Scientific (Pittsburgh, PA).

The use and sources of the affinity purified, rabbit-raised anti-peptide antibodies against the COOH-terminal domain of rat Oat1 (rOat1-Ab; Refs. 2, 22, 24, 37) and Oat3 (rOat3-Ab; Refs. 2, 22, 24) and of the mouse Oat3 (mOat3-Ab; Ref. 28) proteins have been previously described. Instead of using commercial rOat3-Ab, which in the mouse kidney stained the BLM of various nephron segments (2), here we used our noncommercial antibody previously proven in various rat organs (22, 24), which in preliminary studies in the mouse kidney gave the staining pattern identical to that obtained with the commercial one (data not shown). Amino acid sequences of immunizing peptides used for production of these antibodies, as well as alignments of immunizing peptides with the related mOat1 and mOat3 protein domains, are shown in Table 1. A commercial monoclonal antibody for actin (MAB1501R) was purchased from Chemicon. Secondary antibodies, e.g., the CY3-labeled (GARCY3) and alkaline phosphatase-labeled (GARAP) goat anti-rabbit IgG, and fluorescein-labeled (GAMF) and alkaline phosphatase-labeled goat anti-mouse IgG (GAMAP), were purchased from Jackson ImmunoResearch Laboratories (West Grove, PA).

RNA isolation and end-point RT-PCR. After an animal was euthanized by cervical dislocation, both kidneys and largest liver lobe were promptly removed, cut in smaller slices, and immediately submerged into RNAlater solution (Sigma-Aldrich). Total cellular RNA from corresponding tissue slices was extracted using Trizol (Invitrogen, Karlsruhe, Germany) according to the manufacturer's instructions. RNA concentration and its purity were estimated by the spectrophotometric measurement of optical density at 260 and 280 nm (BioSpec Nano, Shimadzu, Japan). The quality and integrity of RNAs were verified by agarose gel electrophoresis, and isolated RNAs were then stored at -70°C until further use. First-strand cDNA synthesis was performed by High-Capacity cDNA Reverse Transcription Kits (Applied Biosystems, Foster City, CA) in accordance with manufacturer's guidelines. Synthesized cDNAs were stored at -20°C until use. PCR was performed in total volume of 20 μ l using: 1 μ l of first-strand cDNA (80 ng), 0.4 μ M specific primers, 0.2 mM dNTP mix, 1 \times PCR buffer, and 0.025 U/ μ l AmpliTaq DNA polymerase (Applied Biosystems) following instructions by the manufacturer. To avoid amplifi-

Table 1. Amino acid sequences of immunizing peptides and alignment of proteins with immunizing peptide of corresponding antibodies used in immunolocalization study

Antibody (Ab)	Immunizing Peptide and References	Ref. Seq. Access. No. of Protein	Alignment of Immunizing Peptides and Respective Protein Sequences
rOat3-Ab	EAEKASQIPLKTGG (22, 24)	NP_112471.2 (mOat3, Slc22a8)	IP 1 EAEKASQIPLKTGG 15 mOat3 522 EAEKASQ T IPLKTGG 536
mOat3-Ab	KASQTIPLKTGDPS (28, 38)	NP_112471.2 (mOat3, Slc22a8)	IP 1 KASQTIPLKTGDPS 14 mOat3 525 KASQTIPLKT G GP 537
rOat1-Ab	MMPLQASTQEKNGL (24)	NP_032792 (mOat1, Slc22a6)	IP 1 MMPLQASTQEKNGL 14 mOat1 532 M I PLQVSTQEKNGL 545

Amino acid sequences of immunizing peptides (IP) and respective sequences in the proteins were aligned by the public BLAST software (<http://blast.ncbi.nlm.nih.gov>) to illustrate the homology between immunizing peptides and target proteins. The underline, bolded amino acids in mOat1 and mOat3 proteins denote amino acids, which are different from those in the corresponding immunizing peptides. Reference Sequence Accession Numbers (Ref. Seq. Access. No.) for mOat1 and mOat3 proteins were identified in the public database (<http://www.ncbi.nlm.nih.gov/protein>).

cation of genomic DNA, intron over-spanning primers were used. Custom primers for *mOat3* and the housekeeping gene ribosomal protein large P2 (*mRplp2*) were created by the public software Primer 3.0 (<http://frodo.wi.mit.edu/primer3/>) and were purchased from Invitrogen (online). The sequences of specific primers used for end point RT-PCR and predicted RT-PCR product sizes are defined in Table 2. Reaction conditions used for PCR were as follows: initial denaturation for 3 min at 94°C, denaturation for 30 s at 95°C, annealing for 30 s at 57°C and elongation for 45 s at 72°C. Experimentally determined optimal PCR cycle numbers were 30 for both *mOat3* and *mRplp2*. Nontemplate control reactions, where the cDNA was substituted with DNase/RNase free water, gave no PCR products, thus indicating the absence of possible contamination (data not shown). RT-PCR products were resolved by electrophoresis in 1% agarose gel, stained with ethidium bromide, and visualized under ultraviolet light.

Tissue fixation and fluorescence immunocytochemistry. Mice were killed by cervical dislocation and bled by cutting the abdominal aorta under a stream of running water. Kidneys were removed, cut in a few sagittal slices, fixed by immersion in 4% *p*-formaldehyde overnight, washed with four abundant volumes of PBS, and stored in PBS (+0.02% NaN₃) until used. Further steps, such as cutting of 4- μ m thick tissue cryosections, optimal antigen retrieval methods for unmasking hidden antigens, blocking with albumin solution, as well as incubation with optimal dilutions of primary and secondary antibodies were described in detail elsewhere (6, 24). The optimal antigen retrieval for Oat3 and actin epitopes included microwave oven heating in 10 mM citrate buffer, pH 6, whereas the optimal antigen retrieval method for Oat1 epitopes included pretreatment of cryosections with xylool and graded concentrations of ethanol (steps used for antigen retrieval in paraffin sections), followed by microwave oven heating in 10 mM citrate buffer, pH 6 (6). To test the specificity of an antibody for the immunizing peptide, the primary antibody was blocked with the respective immunizing peptide (final concentration: 0.5 mg/ml) for 4 h at room temperature before use in immunocytochemistry. The stained sections were examined with an Opton III RS fluorescence microscope (Opton Feintechnik, Oberkochen, Germany) using a Spot RT Slider digital camera and software (Diagnostic Instruments, Sterling Heights, MI). In tissue cryosections from the same experimental group of animals, the photos were taken using the identical microscope and camera settings and were imported into Adobe Photoshop 6.0 software for processing, assembling, and labeling. The intensity of CY3 fluorescence (pixel intensity) was measured in the original images using the IPLab imaging software (BioVision Technologies). One cryosection per kidney from each animal (4 animals in each experimental group) was stained, and three to four representative images with the objective No. 25 were taken from each cryosection. In each image, the background fluorescence in empty peritubular space was subtracted first, the three representative regions of interest (ROI; with 10–15 stained tubule profiles) were then encircled, the average fluorescence pixel intensity in each ROI was measured, and the medium value of all three measurements was calculated. This value was subtracted for the average pixel intensity from three ROI with unstained tubule profiles. These results, obtained from measurements in all three to four images per kidney from one animal, were averaged and used as one datum. The final data are expressed relative to the strongest fluorescence pixel intensity (= 1 relative fluorescence unit) measured in the kidney sections from control male mice. In

representative images shown in figures, the CY3-related red fluorescence was converted into black and white mode using Adobe Photoshop 6.0 software.

To perform double staining of mOat3 and actin, and of mOat1 and actin, the kidney cryosections were first stained for Oat3 or Oat1 proteins as described above and then incubated with the actin-Ab (1:50) at 4°C overnight, washed, and incubated with GAMF (1:100) at room temperature for 60 min. The stained sections were examined, and the images were collected as described above. The images with CY3-related red and fluorescein-related green fluorescence were imported, merged, and processed in Adobe Photoshop.

Preparation of total cell membranes and Western blotting. Mice were killed by cervical dislocation and bled by cutting the abdominal aorta. Kidneys were removed, decapsulated, and minced with scissors, whereas the largest liver lobe was removed and minced. Tissues were homogenized, and total cell membranes (TCM; pellet between 6,000 and 150,000 *g*) were isolated by differential centrifugation as described in detail previously (5). Protein in preparations of TCM was determined by the Bradford assay (3) and adjusted to the desired concentration, and the membranes were stored at -70°C until further use for Western blot analysis.

SDS-PAGE and Western blotting of isolated TCM were described in detail previously (5, 24). Briefly, TCM were mixed with Laemmli buffer under nonreducing conditions and denatured at 37°C for 30 min. Proteins were separated through 10% SDS-PAGE mini gels, and then electrophoretically wet transferred to the Immobilon membrane (Millipore, Bedford, MA). Further handling of the membrane, such as blocking in blotto-buffer, incubation with optimal dilutions of primary and secondary antibodies, as well as visualization of the labeled protein bands with the alkaline phosphatase-mediated reaction, were described in detail in our recent publication (5). To show specificity of the primary antibodies for their epitopes, the antibodies were preincubated with the corresponding immunizing peptides (final concentration: 0.5 mg/ml) for 4 h at room temperature before use in Western blotting. The relative molecular mass (M_r) of the labeled protein bands was estimated by using PageRuler Unstained Protein Ladder (Fermentas, Ontario, Canada). The labeled protein bands were scanned, and their intensity was determined by densitometry using freely available ImageJ software and expressed relative to the strongest band (= 1) in adult intact or castrated male mice.

Presentation of the data and statistical analysis. Images of immunocytochemical and Western blot analysis represent findings in tissue cryosections and membrane samples, respectively, from three to four animals in each experimental group. Quantitative data are expressed as means \pm SE and were statistically evaluated by using either Student's *t*-test or ANOVA with Duncan test at the 5% level of significance by using Statistica 10 software (StatSoft, Tulsa, OK).

RESULTS

Characterization of rOat3-Ab by fluorescence immunocytochemistry in Oat3 KO mouse model. Since the specificity of rOat3-Ab, used in previous studies (2, 18), has not been properly verified, we compared immunolocalization of the Oat3 protein in the kidneys of WT and *Oat3* KO mice (Fig. 1). After the optimal antigen retrieval conditions were applied, in

Table 2. Primer sequences used for RT-PCR

Gene	Forward (F)/Reverse (R) Primers (5'-3')	Ref. Seq. Access. No. of cDNA	Location	RT-PCR product size, bp
<i>mOat3</i>	F:GGCCATCTCATCAACAAC R:AACCAGGCCAGAGAGACA	NM_031194.5	927–946 1,292–1,311	385
<i>mRplp2</i>	F:TACGTCGCCTTACCTGCT R:AACAAGCCAAATCCCATGTC	NM_026020.6	66–85 381–400	335

Ref. Seq. Access. No. for *mOat3* and *mRplp2* cDNAs were identified in the public database (<http://www.ncbi.nlm.nih.gov/gene>).

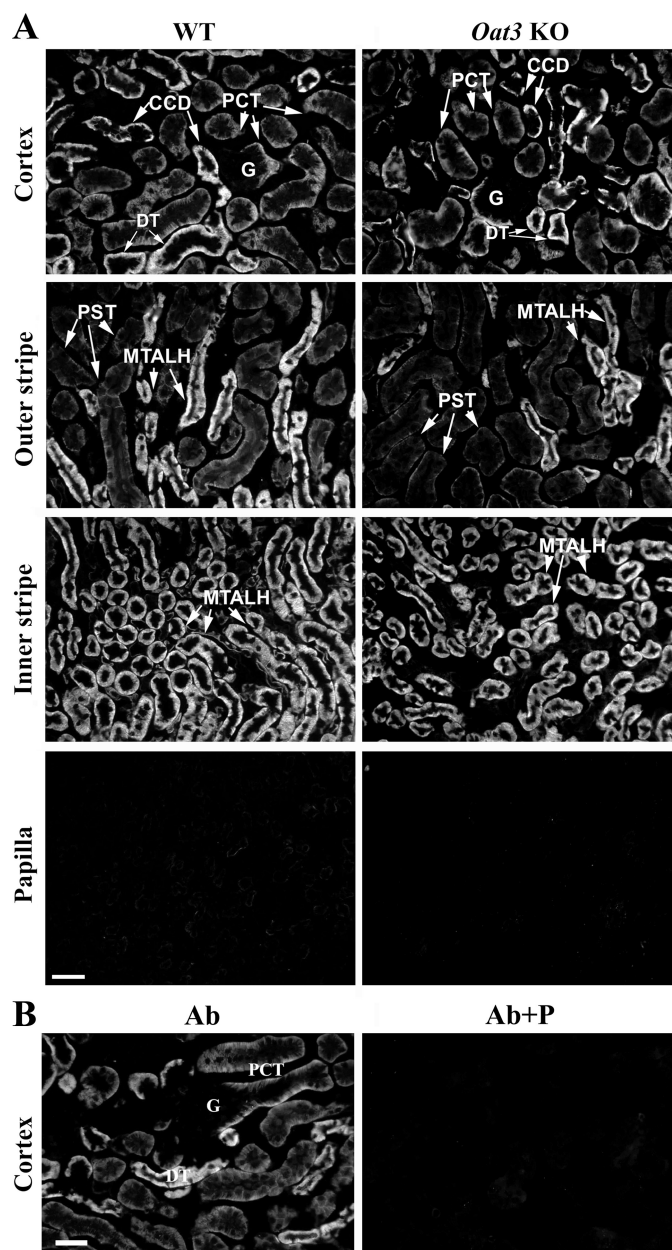


Fig. 1. rOat3-Ab-related immunostaining in cryosections of formalin-fixed kidneys from wild-type (WT) and *Oat3* knockout (KO) male mice. **A**: in the kidney of WT mice, the rOat3-Ab stained the basolateral membrane (BLM) of proximal convoluted tubules (PCT), distal tubule (DT) and cortical collecting duct (CCD) in cortex, of proximal straight tubules (PST) and medullary thick ascending limb (MTALH) in outer stripe, and of medullary thick ascending limb (MTALH) in inner stripe. Glomeruli (G) in cortex and various nephron segments in papilla remained unstained. The same staining pattern was noted in the kidney of *Oat3* KO mice. **B**: in the kidney of *Oat3* KO mice, the rOat3-Ab-related immunostaining (Ab) was absent with the peptide-blocked antibody (Ab + P). Similar results were obtained with WT kidney (not shown). Bar = 20 μ m.

cryosections of the kidneys from WT mice, the rOat3-Ab strongly stained the BLM of epithelial cells along the whole proximal tubule (S1, S2, and S3 segments), TALH, DT, and CCD (Fig. 1A, WT). However, the same immunostaining was observed in cryosections of the kidneys from *Oat3* KO mice (Fig. 1A, *Oat3* KO). In both cases, the rOat3-related immuno-

staining was blocked after preincubation of the antibody with its immunizing peptide (Fig. 1B, Ab + P). These data thus indicate that the rOat3-Ab, which is generated against the rat peptide that differs from the respective sequence in the mouse protein in only one amino acid (Table 1), is not specific for Oat3 protein in mouse organs and, consequently, cannot be used for immunolocalization studies in mice.

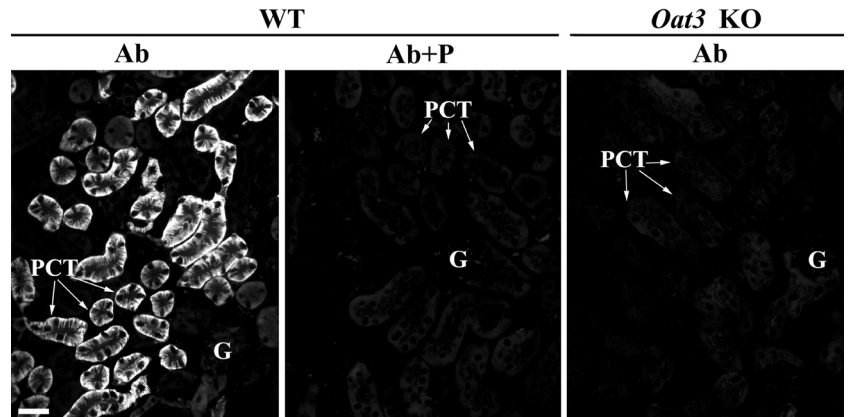
Characterization of mOat3-Ab by fluorescence immunocytochemistry and Western blotting in *Oat3* KO mouse model. We compared localization of the Oat3 protein in the kidneys of WT and *Oat3* KO mice with the mOat3-Ab that was generated against the COOH-terminal domain of the mouse Oat3 protein (Table 1). With the use of optimal antigen retrieval, in cryosections of the kidneys from WT mice the mOat3-Ab strongly stained the BLM of PCT (Fig. 2, WT, Ab). This staining was blocked by the immunizing peptide (Fig. 2, WT, Ab + P). However, in *Oat3* KO mice, no mOat3-Ab-related staining was observed in PCT (Fig. 2, *Oat3* KO, Ab). These data thus indicate that the mOat3-Ab is specific and, therefore, can be used for immunolocalization of the Oat3 protein in mouse organs.

In Western blot analysis, the specificity of mOat3-Ab was tested by labeling protein bands in TCM isolated from the kidneys and liver of WT and *Oat3* KO mice (Fig. 3), where liver was used as an organ in which the expression of Oat3 was not expected (4, 21, 29, 36). In the renal TCM from WT mice, the mOat3-Ab labeled two protein bands of \sim 40 and \sim 70 kDa (Fig. 3A, WT, K), while in the liver TCM from WT mice, it labeled only the \sim 40 kDa band (Fig. 3A, WT, L). Both protein bands were abolished when the mOat3-Ab was preincubated with the immunizing peptide (data not shown). However, in TCM isolated from the kidneys (Fig. 3A, *Oat3* KO, K) and liver (Fig. 3A, *Oat3* KO, L) of *Oat3* KO mice, the mOat3-Ab strongly labeled only the \sim 40 kDa band, indicating that this band was not mOat3 related. On the other hand, the \sim 70 kDa protein band was present in the renal TCM from WT mice and absent in the renal TCM from *Oat3* KO mice, which indicates that this band was mOat3 specific. In addition to these immunohistochemical findings, we have tested the expression of *mOat3* mRNA in the kidneys and liver of WT mice by end-point RT-PCR analysis. As shown in Fig. 3B, and in accordance with previously reported data (4, 21, 29, 36), *mOat3* mRNA was highly expressed in the kidneys but not in the liver of WT mice, thus confirming the \sim 40 kDa protein band as being mOat3 unrelated.

Distribution of the mOat3 protein along the mouse nephron. Since the previously described cell localization of mOat3 in the mouse kidney, as performed with the rOat3-Ab, is obviously incorrect (Fig. 1), we have reinvestigated the cell localization of Oat3 protein along the mouse nephron using the mOat3-Ab. As shown in Fig. 4, in the kidney cortex of WT mice, the mOat3 protein was detected in the BLM of PCT with heterogeneous intensity; the initial S1 segments were not stained; other PCT profiles were strongly stained, whereas the proximal straight tubules (PST; S3 segments) were weakly stained in medullary rays but remained unstained in the outer stripe. Other, more distal segments of the mouse nephron were Oat3 negative.

To confirm localization of the mOat3 protein in proximal tubules, we performed double staining of the kidney cryosections from WT female mice with the mOat3-Ab and actin-Ab.

Fig. 2. mOat3-Ab-related immunostaining in cryosections of formalin-fixed kidneys from WT and *Oat3* KO mice. In the kidney cortex of WT mice, the mOat3-Ab strongly stained the BLM of PCT, whereas glomeruli and other nephron segments remained unstained (Ab). Immunostaining was absent in the kidney from *Oat3* KO mice (Ab) or after applying the immunizing peptide-blocked mOat3-Ab to WT kidney (Ab + P). Bar = 20 μ m.



As shown in Fig. 5, the actin-Ab strongly stained the actin-rich BBM along the whole proximal tubule, including PCT (S1 and S2 segments) and PST (S3 segments; actin, green fluorescence). The mOat3 protein was stained in the BLM of cortical proximal tubules, strongly in most PCT profiles, and weakly in PST (S3 segments) in medullary rays, whereas the initial PCT

(S1 segments) and PST (S3 segments) in the outer stripe remained unstained (Fig. 5, mOat3, red fluorescence). The merged images (merged: actin + mOat3) revealed colocalization of the mOat3-Ab-related BLM staining and the actin-Ab-related BBM staining in most PCT profiles (probably S2 segments) and PST (S3 segments) in medullary rays, whereas the initial (S1) proximal tubule segments in the cortex and S3 segments in the outer stripe, all expressing an actin-rich high brush-border, were Oat3 negative. However, we cannot exclude the possibility that the late S1 segments are also Oat3 positive. As documented previously in C57/BL/6J mice, the height of brush-border along the mouse proximal tubule is approximately the same in all three segments (41), and based on actin staining we are not able to discriminate if the strong Oat3-positive staining in various PCT profiles belongs exclusively to the S2 segments or also to the late part of S1 segments. However, this colocalization study undoubtedly confirmed that, in the mouse kidney, the mOat3 protein is localized in the BLM of proximal tubule S2 and S3 segments in the cortex and not in other parts of the nephron.

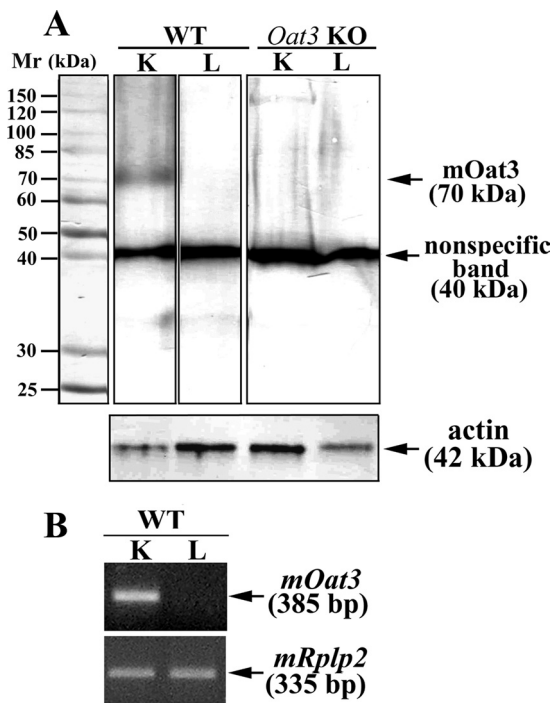
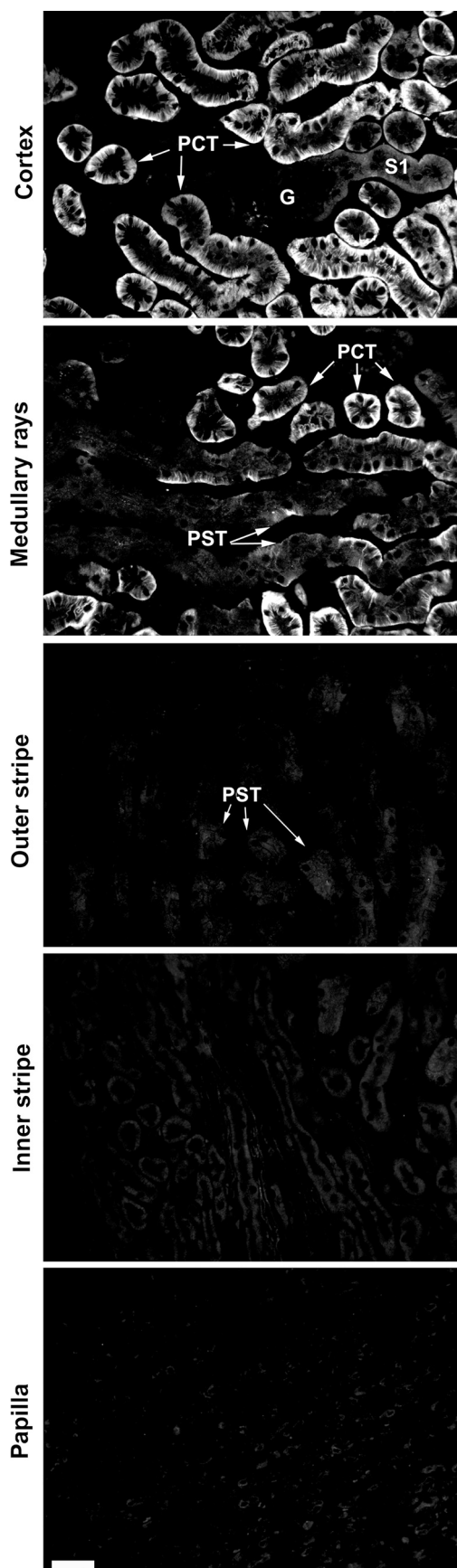


Fig. 3. Testing the mOat3-Ab specificity in *Oat3* KO mouse model with Western blotting of isolated renal and liver total cell membranes (TCM; A) and RT-PCR analysis of *mOat3* mRNA in the kidney and liver of WT mice (B). A: in TCM isolated from the whole kidneys (K) of WT mice, the mOat3-Ab labeled two protein bands of relative molecular mass (M_r) \sim 40 kDa (stronger) and \sim 70 kDa (weaker). However, in the renal TCM from *Oat3* KO mice, the \sim 70 kDa band was absent, whereas the \sim 40 kDa band remained strong. In the liver (L), TCM from both animal groups only the strong \sim 40 kDa band was detected. All TCM samples were run on the same SDS-PAGE gel, but some unnecessary lanes were removed for the final presentation. Each lane contained 40 μ g of protein, but the 42 kDa band of actin, used here as a loading control, was heterogeneous in density. B: end-point RT-PCR analysis of *mOat3* mRNA in the liver (L) and kidney (K) tissue of WT mice. The specific *mOat3*-related RT-PCR product of 385 bp was detected only in the kidney, whereas the expression of *mRplp2*-related RT-PCR product of 335 bp was similar in both organs indicating similar cDNA input.

In view of the data showing that the functionally similar transporter Oat1 exhibits localization in proximal tubule of the mouse (18) and rat (24) kidneys similar to that of Oat3, we have tested distribution of the mOat1 protein in the kidneys of WT male mice in colocalization with actin. As shown in Fig. 6 (actin, green fluorescence), the actin-Ab strongly stained a high BBM of the entire proximal tubule in the cortex and outer stripe. However, the mOat1-Ab (red fluorescence) did not stain the initial part of PCT (S1 segments), but it stained strongly the BLM of most PCT profiles and weakly the BLM of PST (S3 segments) in medullary rays, whereas S3 segments in the outer stripe remained unstained. The merged image clearly indicates that the mOat1 protein is localized in the BLM of proximal tubule S2 (possibly also in the late portion of S1 segments) and S3 segments in the cortex (Fig. 6, merged: mOat1 + actin). This and the preceding colocalization study further indicate that both mOat3 and mOat1 proteins are localized in the BLM of the same proximal tubule segments (S2 and S3) in the cortex, whereas other parts of the mouse nephron are devoid of both transporters.

Sex-dependent expression of renal mOat3 protein; effect of castration and treatment with sex hormones. It was previously shown that the expression of *mOat3* mRNA in the mouse kidney is sex dependent (9, 15, 39), but the sex-related expression of mOat3 protein has not been reported. Thus, to demon-



strate possible sex differences, we performed immunochemical analysis with the mOat3-Ab in the kidneys of adult WT male and female mice. As shown in Western blots and densitometric evaluation of the labeled bands (Fig. 7, *A* and *B*, respectively), in isolated renal TCM, the relative amount of the mOat3 protein band of ~70 kDa band was approximately twofold stronger in females than in males, whereas the density of the 110 kDa band of Na-K-ATPase exhibited no sex differences. The immunocytochemical data corroborated the Western blotting data; in cryosections of the mouse kidney cortex, the mOat3-related fluorescence intensity in the BLM of PCT was approximately twofold stronger in females than in males (Fig. 7, *C* and *D*). These protein data are thus in agreement with the previously reported female-dominant expression of *mOat3* mRNA (9, 15, 39).

To reveal effects of androgen hormones on the renal mOat3 protein expression, male mice were sham operated or castrated at the age of 2 mo, and 1 mo later the expression of mOat3 protein was tested by immunochemical methods as shown in Fig. 8. In isolated renal TCM, castration markedly (~2.5-fold) upregulated the abundance of mOat3 protein band of ~70 kDa, whereas the 110 kDa protein band of Na-K-ATPase remained unaffected (Fig. 8, *A* and *B*). The immunocytochemical data exhibited a pattern comparable to that of Western blots; the mOat3-related fluorescence intensity in the BLM of PCT was ~2.5-fold stronger in castrated than in sham-operated males (Fig. 8, *C* and *D*). These data indicate that the female-dominant expression of renal mOat3 in adult mice is caused by inhibitory effects of androgens. To confirm the androgen-dependent effect on the mOat3 protein expression, castrated mice were treated with either oil (controls) or testosterone, or estradiol for 2 wk, and the mOat3 protein expression was determined by immunochemical methods as shown in Fig. 9. In isolated renal TCM, testosterone treatment strongly (~85%) downregulated the abundance of the mOat3 protein band of ~70 kDa, compared with oil-treated castrates, whereas estradiol treatment had no effect. The relative expression of the Na-K-ATPase protein band of 110 kDa was unaffected by both sex hormones (Fig. 9, *A* and *B*). The immunoblotting data were supported by similar pattern of the immunostaining data in tissue cryosections: the mOat3-related fluorescence intensity in the BLM of PCT was strongly diminished only in testosterone-treated castrates; estradiol had no significant effect (Fig. 9C). This experiment thus confirmed that the renal expression of mOat3 protein in mice is inhibited by androgens.

Sex-dependent expression of renal mOat1 protein; effect of castration and treatment with sex hormones. Previous data indicated that the expression of renal mOat1 is male dominant at both mRNA (9, 15, 18, 39) and protein (18) levels. To support these data, we investigated the expression of renal mOat1 protein by our immunochemical methods. As shown in Fig. 10, *A* and *B*, the abundance of mOat1 protein in isolated renal TCM was approximately fourfold higher in males than in females. The intensity of mOat1-related immunostaining in

Fig. 4. mOat3-Ab-related immunostaining along the mouse nephron. Antibody stained strongly the BLM of PCT and weakly the BLM of PST in medullary rays, whereas the initial portion of S1 segments and PST in the outer stripe were unstained. No staining was observed in glomeruli (G) and distal nephron segments in the inner stripe and papilla. Bar = 20 μ m.

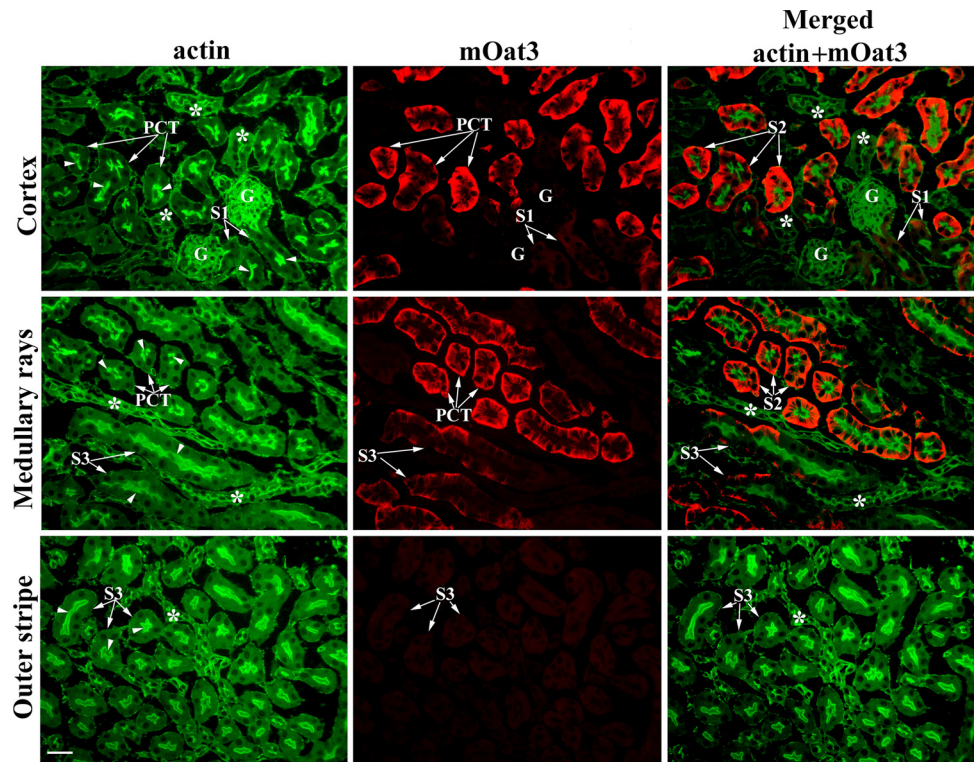


Fig. 5. Double immunostaining in cryosections of the formalin-fixed kidneys from WT female mice with actin-Ab and mOat3-Ab. Actin-Ab (green fluorescence) strongly stained the tall brush border membrane (BBM; arrows) of PCT (S1 and S2 segments) and straight (PST; S3 segments) tubules, whereas more distal nephron segments (*) and various peritubular structures were weaker stained. mOat3-Ab (red fluorescence) stained strongly the BLM of PCT and weakly the BLM of PST in medullary rays, whereas the initial S1 segments next to the glomeruli and S3 segments in the outer stripe were Oat3 negative. Merged image (green + red fluorescence) shows colocalization of mOat3 and actin proteins in PCT (mainly S2 segments) and PST (S3 segments) in medullary rays. Initial proximal tubule segments (S1) in the cortex and S3 segments in the outer stripe, as well as the actin-positive distal nephron segments (*) and various peritubular structures, are Oat3 negative. Bar = 20 μ m.

cryosections of the kidney cortex matched the WB data; the staining intensity in the BLM of PCT was \sim 3.2-fold stronger in males than in females (Fig. 10, C and D).

As shown in Fig. 11, A and B, castration in males markedly (\sim 50%) decreased the density of the mOat1 protein band of \sim 75 kDa in isolated renal TCM, whereas the abundance of

Na-K-ATPase was not affected. The immunocytochemical data confirmed the Western blot results; the intensity of mOat1-related immunostaining in castrated males was for 60% weaker than in sham-operated males (Fig. 11, C and D). These data indicate that the male-dominant expression of renal mOat1 in adult mice is due to stimulatory effects of androgens. In

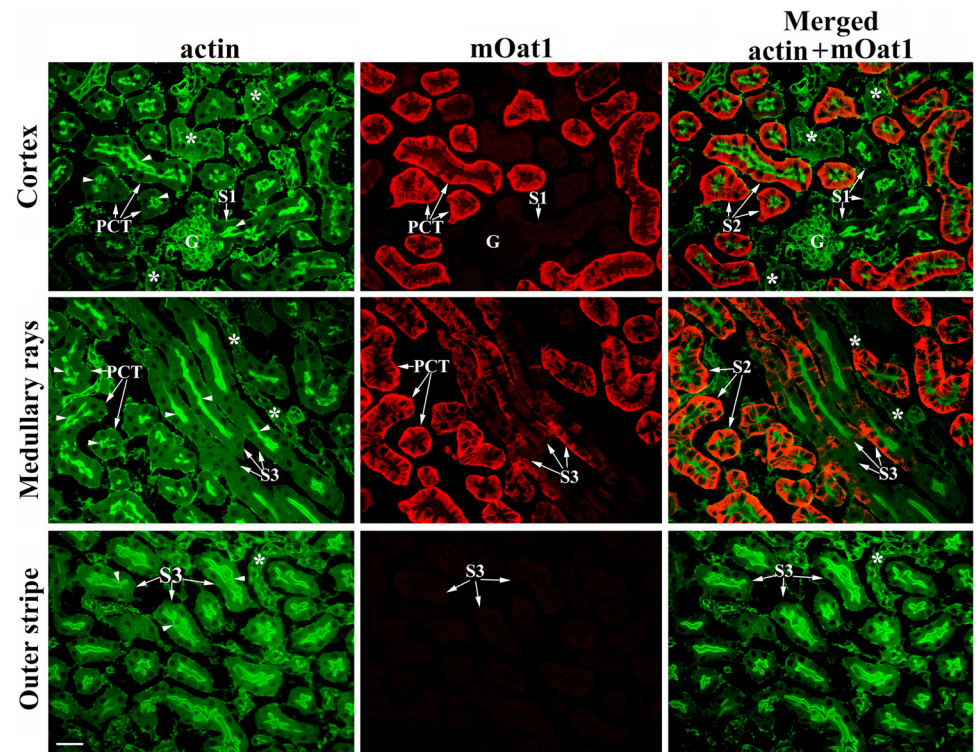


Fig. 6. Double immunostaining in cryosections of the formalin-fixed kidneys from WT male mice with actin-Ab and rOat1-Ab. Actin-Ab (green fluorescence) strongly stained the tall BBM (arrows) of PCT (S1 and S2 segments) and straight (PST; S3 segments) tubules, whereas more distal nephron segments (*) and various peritubular structures were weaker stained. rOat1-Ab (red fluorescence) stained strongly the BLM of PCT and weakly the BLM of PST (S3 segments) in medullary rays, whereas the initial, S1 segments next to the glomeruli and S3 segments in the outer stripe, were Oat1 negative. The merged image (green + red fluorescence) shows colocalization of mOat1 and actin proteins in PCT (mainly S2 segments) and PST (S3 segments) in medullary rays. Initial proximal tubule segments (S1) in the cortex and S3 segments in the outer stripe, as well as the actin-positive distal nephron segments (*) and various peritubular structures, are Oat1 negative. Bar = 20 μ m.

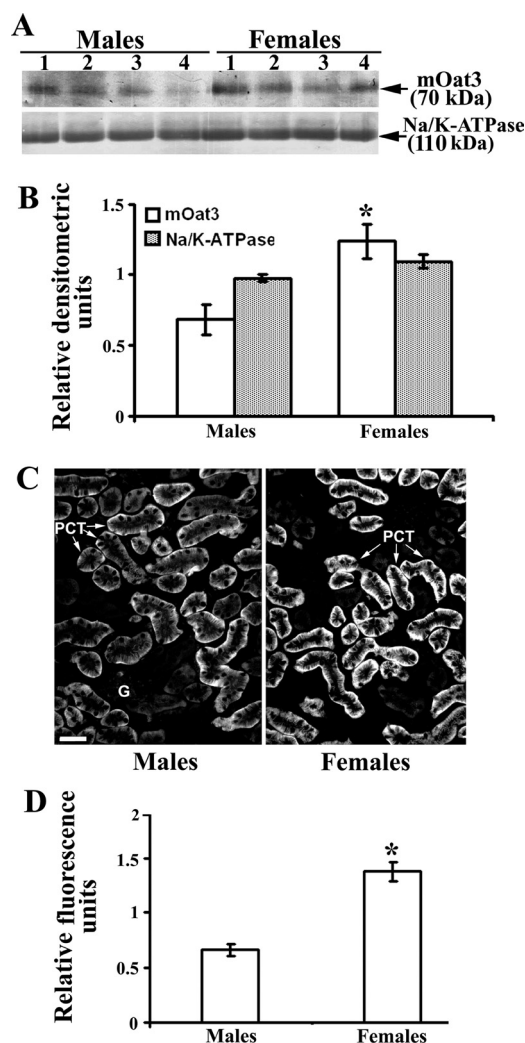


Fig. 7. Sex-dependent expression of the renal mOat3 protein in adult mice: Western blot (A and B) and immunocytochemical (C and D) analysis. A: Western blot of renal TCM with mOat3-Ab and Na-K-ATPase-Ab in adult males and females. B: densitometric evaluation of the same bands. Relative amount of the mOat3-related protein band of ~70 kDa was ~2-fold stronger in females than in males, whereas the relative amount of the 110 kDa band of Na-K-ATPase was similar in both sexes, indicating similar protein loading. Each lane contained 80 μ g of protein. Each bar is means \pm SE of the data from 4 independent TCM preparations. * P < 0.05 vs. males. C: mOat3-Ab-related immunostaining in the cortex of formalin-fixed mouse kidneys from adult male and female mice. D: level of fluorescence pixel intensity in the BLM of PCT; the staining intensity in females was ~2-fold stronger than in males. Bar = 20 μ m. Each bar is the means \pm SE of the data in cryosections from 4 animals in each group. * P < 0.05 vs. males.

support of these findings, castrated mice were treated with oil (controls) or testosterone, or estradiol for 2 wk, and the mOat1 protein expression was determined by immunochemical methods as shown in Fig. 12. In isolated renal TCM, testosterone treatment markedly (~2.5-fold) upregulated the abundance of the mOat1 protein band of ~75 kDa, compared with oil-treated castrates, whereas estradiol treatment had no effect. The relative amount of the Na-K-ATPase protein band of 110 kDa was not affected by sex-hormone treatment (Fig. 12, A and B). By immunostaining in tissue cryosections, the mOat1-related fluorescence intensity in the BLM of PCT was stronger in testosterone treated than in oil-treated castrates, whereas estra-

diol treatment had no effect (Fig. 12C). These data thus confirmed that the renal expression of mOat1 protein in mice is stimulated by androgens.

DISCUSSION

In this study we used an *Oat3* KO mouse model and adult WT male and female mice, as well as sex hormone-treated castrated WT mice to execute several tasks: 1) to verify the previously reported localization of Oat3 protein along the mouse nephron by testing two different polyclonal antibodies

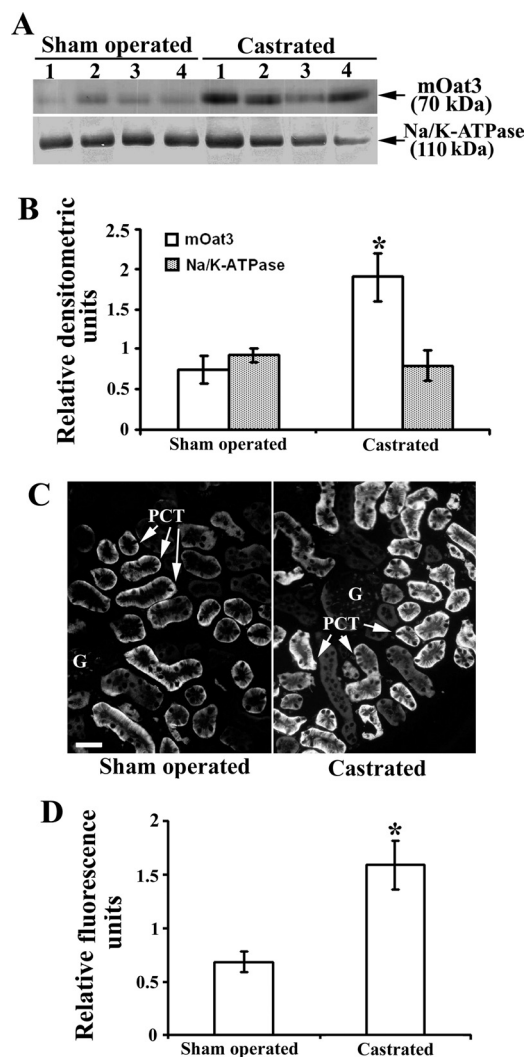


Fig. 8. Expression of the renal mOat3 protein in adult male mice—effect of castration: Western blot (A and B) and immunocytochemical (C and D) analysis. A: Western blot of the renal TCM with mOat3-Ab and Na-K-ATPase-Ab in adult sham-operated and castrated males. B: densitometric evaluation of the same bands. The ~70 kDa protein band was ~2.5-fold stronger in castrated than in sham-operated males, whereas the relative expression of Na-K-ATPase remained unaffected by castration. Each lane contained 80 μ g of protein. Each bar is the means \pm SE of the data from 4 independent TCM preparations. * P < 0.05 vs. sham operated. C: mOat3-Ab-related immunostaining in cryosections of formalin-fixed kidneys from sham-operated and castrated males. D: level of fluorescence pixel intensity in the BLM of PCT; compared with the sham-operated animals, the staining intensity in castrated animals increased ~2.5-fold. Bar = 20 μ m. Each bar is the means \pm SE of the data in cryosections from 4 animals in each group. * P < 0.05 vs. sham operated.

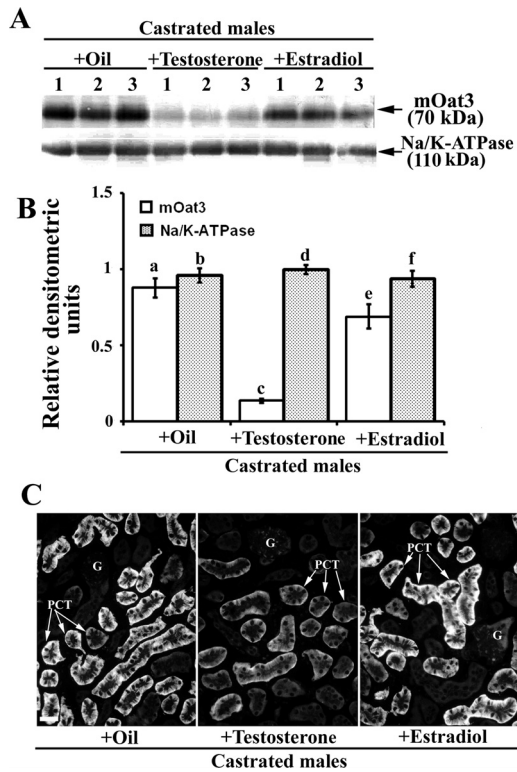


Fig. 9. Expression of the renal mOat3 protein in adult castrated male mice—effects of the treatment with sex hormones: Western blot (A and B) and immunocytochemical (C) analysis. A: Western blot of the renal TCM with mOat3-Ab and Na-K-ATPase-Ab in castrated males treated with oil, testosterone or estradiol. B: densitometric evaluation of the same bands. Compared with the oil-treated castrated mice, testosterone strongly (~85%) decreased, whereas estradiol did not change the expression of the mOat3-related protein band of ~70 kDa. Relative abundance of the Na-K-ATPase protein band of 110 kDa remained unaffected by both hormones, and indicated similar protein loading. Each lane contained 80 μ g of protein. Each bar is the means \pm SE of the data from 3 independent TCM preparations. Statistics: a vs. c and c vs. e, $P < 0.05$; other relations, NS. C: mOat3-Ab-related immunostaining in cryosections of formalin-fixed kidneys from castrated males treated with oil, testosterone or estradiol. Staining intensity completely matched the Western blot data; the testosterone treatment markedly suppressed, whereas the estradiol treatment did not affect the mOat3-related staining intensity in the BLM of PCT in the cortex. Immunocytochemical data represent findings in 3 animals in each experimental group. Bar = 20 μ m.

against the COOH-terminal domain of the rat (rOat3-Ab) and mouse (mOat3-Ab) Oat3 proteins; 2) to test the presence of sex differences in the expression of renal mOat3 protein in view of the previously reported differences in *mOat3* mRNA levels; 3) to test sex differences in the expression of renal mOat1 protein, which colocalizes with mOat3 in the BLM of epithelial cells in specific nephron segments; and 4) to define the hormone(s) responsible for sex differences in the expression of renal mOat3 and mOat1 proteins.

A polyclonal rOat3-Ab was originally designed for immunolocalization studies of the Oat3 protein in rat organs (22, 24). The BLAST analysis indicated that the rOat3-Ab could cross-react with the same protein in mice, and it was thus used previously to localize the Oat3 protein also in the mouse kidney (18). In the present study in WT mice, consistent with the previous findings in rat and mouse kidneys, the rOat3-Ab strongly stained the BLM of proximal tubule segments (S1 < S2 > S3) and of more distal nephron segments, such as TALH,

DT, and CCD. This immunostaining was completely blocked by the immunizing peptide. An unexpected finding with this antibody was an identical, peptide-blockable immunostaining in the kidneys of *Oat3* KO mice, suggesting that in addition to the possibly specific epitope in Oat3 protein, the rOat3-Ab stains some other, non-mOat3 protein(s) and, therefore, is not appropriate for immunolocalization studies in mouse organs. In contrast, the mOat3-Ab, which was designed for immunolocalization studies of the Oat3 protein in mouse organs (28), stained the BLM of proximal tubule in the kidneys of WT mice with the segment-related intensity, whereas distal parts of the

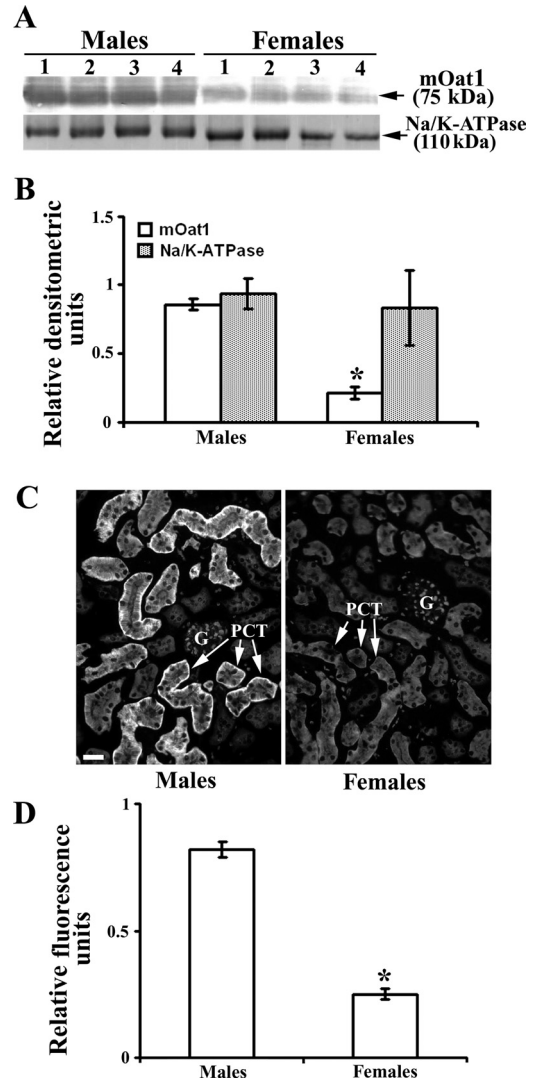


Fig. 10. Sex-dependent expression of the renal mOat1 protein in adult mice: Western blot (A and B) and immunocytochemical (C and D) analysis. A: Western blot of the renal TCM with rOat1-Ab and Na-K-ATPase-Ab in males and females. B: densitometric evaluation of the same bands. mOat1-related protein band of 75 kDa was ~4-fold stronger in males than in females, whereas the 110 kDa band of Na-K-ATPase was similar in all samples indicating similar protein loading. Each lane contained 80 μ g of protein. Each bar is the means \pm SE of the data from 4 independent TCM preparations. * $P < 0.05$ vs. males. C: rOat1-Ab-related immunostaining in the cortex of formalin-fixed mouse kidneys from male and female mice. D: level of fluorescence pixel intensity in the BLM of PCT; the staining intensity was ~3.2-fold stronger in males than in females. Bar = 20 μ m. Each bar is the means \pm SE of the data from kidney cryosections from 4 animals in each group. * $P < 0.05$ vs. males.

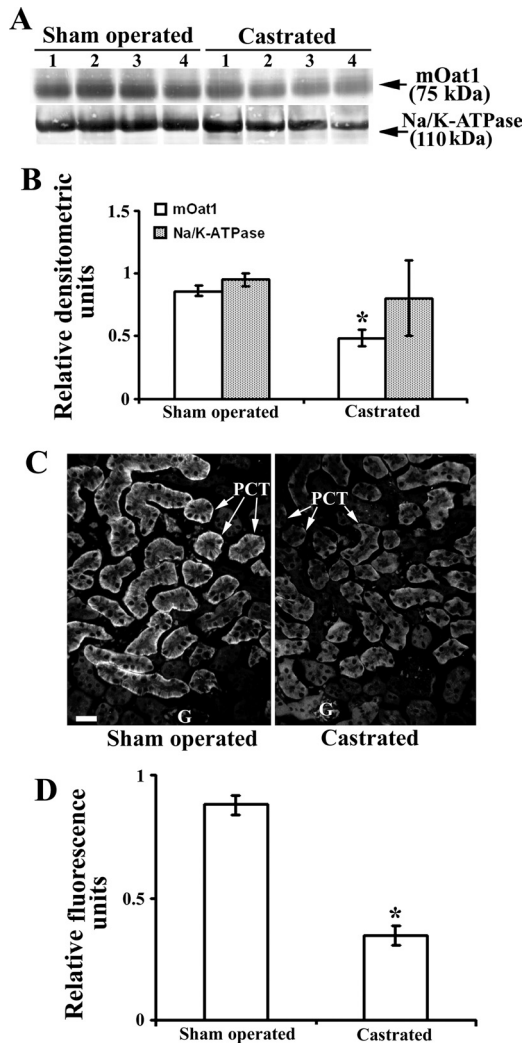


Fig. 11. Expression of the renal mOat1 protein in adult male mouse—effect of castration: Western blot (A and B) and immunocytochemical (C and D) analysis. A: Western blot of the renal TCM with rOat1-Ab and Na-K-ATPase-Ab in sham-operated and castrated males. B: densitometric evaluation of the same bands. The ~75 kDa protein band in castrated males was ~50% weaker than in sham-operated males, whereas the relative expression of Na-K-ATPase remained unaffected by castration. Each lane contained 80 μ g of protein. Each bar is the means \pm SE of the data from 4 independent TCM preparations. * $P < 0.05$ vs. sham operated. C: rOat1-Ab-related immunostaining in cryosections of formalin-fixed kidneys from the sham-operated and castrated males. D: level of fluorescence pixel intensity in the BLM of PCT in castrated animals decreased for ~60%. Bar = 20 μ m. Each bar is means \pm SE of the data in cryosections from 4 animals in each group. * $P < 0.05$ vs. sham operated.

nephron were Oat3 negative. Importantly, no staining was observed with this antibody in renal tubules of *Oat3* KO mice, proving the mOat3-Ab as a specific probe for Oat3 protein in mouse organs. Despite the significant similarity of immunizing peptides, which were used for production of rOat3-Ab and mOat3-Ab (Table 1), our immunocytochemical findings revealed that these two antibodies recognize different epitopes in the mouse kidney. Our data further demonstrated that 1) blocking an antibody with its immunizing peptide does not confirm its specificity; the immunostaining with rOat3-Ab in both WT and *Oat3* KO mice was blocked by the immunizing peptide, and 2) in silico alignment of the immunizing peptide

with the proteins expressed within the whole organism is not verification of the antibody specificity. Taken together, we emphasize the use of an appropriate KO mouse model (where available) as the best experimental test for specificity of an antibody.

In Western blots of the renal and liver TCM from WT and *Oat3* KO mice, the mOat3-Ab labeled two protein bands with M_r of ~40 kDa (stronger) and ~70 kDa (weaker). However, the ~40 kDa band was strongly labeled in the membranes from mOat3-positive (kidneys in WT mice) and mOat3-negative (liver in WT mice and kidneys in *Oat3* KO mice) organs and, therefore, cannot be related to mOat3. The ~40 kDa protein band did not contribute to immunocytochemical staining since no staining was observed with the mOat3-Ab in cryosections from *Oat3* KO mice. On the other hand, the ~70 kDa band was not detected in TCM from the liver of WT mice, which corresponds with the absence of *mOat3* mRNA in this organ

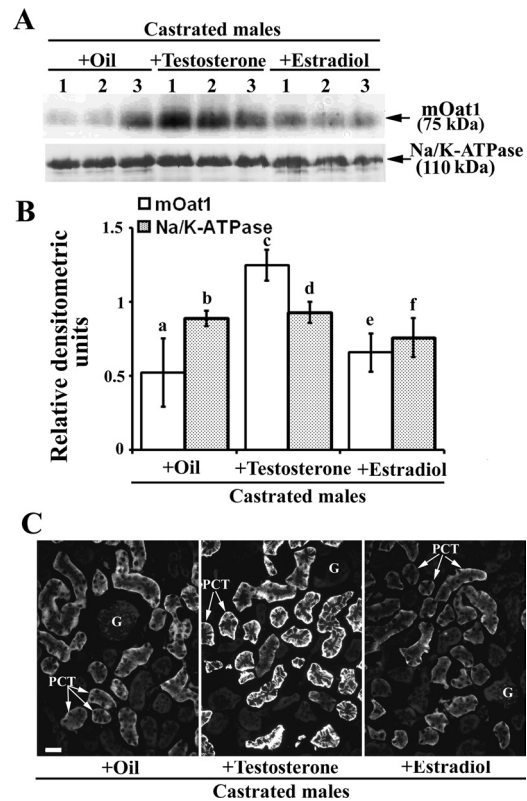


Fig. 12. Expression of the renal mOat1 protein in adult castrated male mice—effects of treatment with sex hormones; Western blot (A and B) and immunocytochemical (C) analysis. A: Western blot of the renal TCM with rOat1-Ab and Na-K-ATPase-Ab in castrated males treated with oil, testosterone and estradiol. B: densitometric evaluation of the same bands. Compared with the oil-treated castrated mice, testosterone strongly increased (~2.4-fold), whereas estradiol did not change, the expression of the mOat1-related protein band of ~75 kDa. The relative density of the Na-K-ATPase protein band of 110 kDa remained unaffected by either sex hormone. Each lane contained 80 μ g of protein. Each bar is the means \pm SE of the data from 3 independent TCM preparations. Statistics: a vs. c and c vs. e, $P < 0.05$; other relations, NS. C: rOat1-Ab-related immunostaining in cryosections of formalin-fixed kidneys from castrated males treated with oil, testosterone or estradiol. Intensity of the mOat1-related fluorescence staining completely matched the Western blotting data; compared with the oil-treated castrates, testosterone treatment markedly increased the staining intensity of the BLM in PCT, whereas the estradiol treatment had no effect. Immunocytochemical data represent findings in 3 animals in each experimental group. Bar = 20 μ m.

(4, 21, 29, 36; and this study), and in TCM from the kidneys of *mOat3* KO mice, and is, therefore, mOat3 specific. Moreover, our RT-PCR data confirmed previous reports that *mOat3* mRNA was predominantly expressed in the mouse kidney, but absent in the mouse liver, and additionally implied that the protein band of ~70 kDa was mOat3 related, whereas the protein band of ~40 kDa was unspecific. The M_r of ~70 kDa is greater than predicted for the mOat3 protein containing 537 amino acid residues (calculated M_r ~59 kDa) and probably represents the glycosylated form. The protein has multiple putative *N*-linked glycosylation sites on the large first extracellular loop (10, 30, 34) and up to four of them may be glycosylated (<http://www.cbs.dtu.dk/services/NetNGlyc/>). Since each *N*-linked sugar contributes to M_r with ~4 kDa, glycosylation can easily explain the differences between the predicted (~59 kDa) and apparent (~70 kDa) M_r of the mOat3 protein. A similar phenomenon was previously observed for hOAT1 (12). Other studies in crude membrane fractions from the mouse kidney and brain described the mOat3-related protein band of ~50 (29) and ~70 kDa (38), whereas in rats, the rOat3-Ab labeled the protein bands between ~55 and ~75 kDa, all being explained with differential, tissue-specific glycosylation (16, 19, 24, 27).

In our hands, in both single- and double-immunostaining modes, the mOat3-Ab strongly stained the BLM of PCT (mainly S2 segments) and weakly stained the BLM of PST (S3 segments) in medullary rays, while the initial S1 segments and S3 segments in the outer stripe were Oat3 negative. Importantly, distal segments of the mouse nephron were also Oat3 negative. Thus with the mOat3-Ab we showed localization of Oat3 protein along the mouse nephron different from that in previous studies (28); using the same antibody, Nilwarangkoon et al. (28) reported mOat3-related staining in the BLM of proximal tubule and of other, more distal nephron segments. The reason for this discrepancy with our data is not clear; we tend to believe that it may be related to the proper method of antigen retrieval in the present study, but we cannot exclude influences of the mouse strain (ICR in previous study and C57Bl/6 in this study) and rodent chow. In addition, previous data were not verified in *mOat3* KO mice. In the rat kidney, with the use of the rOat3-Ab, rOat3 was localized to the BLM of proximal tubules and more distal nephron segments, including TALH, DT, and CCD principal cells (22, 24), whereas in the human kidney, with the use of a hOAT3-Ab, hOAT3 was localized only to the BLM of proximal tubules (11, 26). Therefore, the present data indicate that the distribution of mOat3 and hOAT3 in the respective mammalian nephron is comparable.

In contrast to the renal mOat3 protein, with previously unknown distribution along the mouse nephron, the exact localization of mOat1 in the mouse kidney was previously verified with the rOat1-Ab in *Oat1* KO mouse model (14). Consistent with previous data (2, 14, 18), using an optimal antigen unmasking technique and single- or double-immunostaining modes, we detected the mOat1 protein in the BLM of proximal tubules, where the initial S1 segments were negative, S2 segments were strongly positive, and S3 segments in medullary rays and outer stripe were weakly positive and negative, respectively. The same pattern of Oat1/OAT1 localization along the nephron was found in rat (22, 24, 27) and human (17, 26) kidneys.

Our immunochemical studies in intact male and female mice revealed that mOat3 and mOat1 exhibit opposite sex-dependent patterns of protein expression; the expression of mOat3 protein is female dominant, whereas the expression of mOat1 protein is male dominant. These findings are in agreement with the previously published data on female-dominant expression of *mOat3* mRNA and male-dominant expression of *mOat1* mRNA and protein in mouse kidneys (9, 15, 18, 39). Our experiments in castrated male mice clearly showed that the expression level of both transporters is dependent on androgens but in opposite directions; castration markedly upregulated the expression of mOat3 protein, suggesting an inhibitory effect of androgens on its expression, whereas the expression of mOat1 protein was downregulated by castration, suggesting a stimulatory effect of androgens on its expression. These assumptions were proven in castrated mice treated with specific sex hormones for 2 wk, in which testosterone treatment inhibited the expression of renal mOat3 protein and stimulated the expression of renal mOat1 protein, whereas treatment with estradiol had no significant effect on the expression of either Oat.

Overall, these data are in agreement with numerous previous studies that indicated sex hormones as the key factors in regulation of various Oats at their mRNA and/or protein levels in the rodent liver and kidneys (5, 8, 20, 24, 25, 31, 32), but details of this regulation have been poorly studied. The presence of numerous conserved potential binding sites for transcription factors within the noncoding sequences of mouse Oats has been reported (13). In addition, both the *mOat1* and *mOat3* genes are located on mouse chromosome 19 with an intergenic distance of 7.5-kb pairs, suggesting that the expression of their transcripts and proteins might be tightly coordinated as a pair (13). Recently, Vallon et al. (38) again suggested that the transcription of RNAs and translation of mOat3 and mOat1 proteins may be tightly regulated as a possible consequence of their adjacent chromosomal location. In their study, in *Oat3* KO mice the renal expression of *mOat1* mRNA and its protein was reduced to ~64 and ~60%, respectively, whereas in *Oat1* KO mice, the renal expression of *mOat3* mRNA and its protein was reduced to ~22 and ~6%, respectively, when compared with the expression in WT mice. However, our data showing a completely opposite androgen-dependent expression of these two transporters, as well as the data of Groves et al. (15) and VanWert et al. (39), suggest that *mOat3*/mOat3 and *mOat1*/mOat1 probably are not regulated as a pair at the level of transcription and/or translation. Contrary to the situation in mice, the expression of both Oat1 and Oat3 in rat kidneys exhibits strong male-dominant sex differences at the protein and mRNA levels that appear after puberty and are caused by both stimulatory effects of androgens and inhibitory effects of estrogens (7, 8, 9, 24). Overall, these data indicate the presence of species differences in regulation of transcription and/or translation of the sex hormone-affected genes (32).

In summary, we showed that in the mouse kidney 1) Oat3 is localized in the BLM of cortical proximal tubules with heterogeneous intensity (initial S1 negative; S2 > S3) and thus differs from the widespread localization of Oat3 in the rat kidneys, thus indicating the presence of species differences, and 2) Oat3 and Oat1 proteins colocalize in the same segments of the mouse nephron, where they exhibit opposite patterns of sex-dependent expression; Oat3 expression is female dominant due to androgen inhibition, while Oat1 expression is male

dominant due to androgen stimulation. Knowledge of species and sex differences of specific Oats is important for estimation and interpretation of their relative contribution in ex vivo and in vivo functional assays, since they transport a wide range of overlapping substrates, such as metabolites, drugs, and toxins.

ACKNOWLEDGMENTS

We thank Eva Heršak for technical assistance.

GRANTS

This work was supported by Croatian Ministry of Science, Education and Sports Grant 022-0222148-2146 (to I. Sabolic) and National Institute of Diabetes and Digestive and Kidney Diseases Grant R01-DK-067216 (to D. H. Sweet).

DISCLOSURES

No conflicts of interest, financial or otherwise, are declared by the author(s).

AUTHOR CONTRIBUTIONS

Author contributions: D.B. and I.S. conception and design of research; D.B., H.B., and D.H.S. performed experiments; D.B., D.H.S., N.A., and I.S. analyzed data; D.B. and I.S. interpreted results of experiments; D.B. and H.B. prepared figures; D.B. drafted manuscript; D.B., D.H.S., N.A., and I.S. edited and revised manuscript; I.S. approved final version of manuscript.

REFERENCES

- Anzai N, Kanai Y, Endou H. Organic anion transporter family: current knowledge. *J Pharm Sci* 100: 411–426, 2006.
- Bahn A, Ljubojevic M, Lorenz H, Schultz C, Ghebremedhin E, Ugele B, Sabolic I, Burckhardt G, Hagos Y. Murine renal organic anion transporters mOAT1 and mOAT3 facilitate the transport of neuroactive tryptophan metabolites. *Am J Physiol Cell Physiol* 289: C1075–C1084, 2005.
- Bradford MM. A rapid and sensitive method for the quantitation of microgram quantities of protein utilizing the principle of protein-dye binding. *Anal Biochem* 72: 248–254, 1976.
- Brady KP, Dushkin H, Fornzler D, Koike T, Magner F, Her H, Gullans ST, Segre GV, Green RM, Beier DR. A novel putative transporter maps to the osteosclerosis (oc) mutation and is not expressed in the oc mutant mouse. *Genomics* 56: 254–261, 1999.
- Breljak D, Ljubojevic M, Balen D, Zlender V, Brzica H, Micek V, Kusan M, Anzai N, Sabolic I. Renal expression of organic anion transporter Oat5 in rats and mice exhibits the female-dominant sex differences. *Histol Histopathol* 25: 1385–1402, 2010.
- Brzica H, Breljak D, Ljubojevic M, Balen D, Micek V, Anzai N, Sabolic I. Optimal methods of antigen retrieval for organic anion transporters in cryosections of the rat kidney. *Arh Hig Rada Toksikol* 60: 7–17, 2009.
- Buist SCN, Cherrington NJ, Choudhuri S, Hartley DP, Klaassen CD. Gender-specific and developmental influences on the expression of rat organic anion transporters. *J Pharmacol Exp Ther* 301: 145–151, 2002.
- Buist SCN, Cherrington NJ, Klaassen CD. Endocrine regulation of rat organic anion transporters. *Drug Metab Dispos* 31: 559–564, 2003.
- Buist SCN, Klaassen CD. Rat and mouse differences in gender-predominant expression of organic anion transporter (OAT1-3; SLC22A6-8) mRNA levels. *Drug Metab Dispos* 32: 620–625, 2004.
- Burckhardt BC, Burckhardt G. Transport of organic anions across the basolateral membrane of proximal tubule cells. *Rev Physiol Biochem Pharmacol* 146: 95–158, 2003.
- Cha SH, Sekine T, Fukushima JI, Kanai Y, Kobayashi Y, Goya T, Endou H. Identification and characterization of human organic anion transporter 3 expressing predominantly in the kidney. *Mol Pharmacol* 59: 1277–1286, 2001.
- Cihlar T, Lin DC, Pritchard JB, Fuller MD, Mendell DB, Sweet DH. The antiviral nucleotide analogs cidofovir and adefovir are novel substrates for human and rat renal organic anion transporter. *Mol Pharmacol* 56: 570–580, 1999.
- Eraly SA, Hamilton BA, Nigam SK. Organic anion and cation transporters occur in pairs of similar and similarly expressed genes. *Biochem Biophys Res Commun* 300: 333–342, 2003.
- Eraly SA, Vallon V, Vaugh DA, Gangoiti JA, Richter K, Nagle M, Monte JC, Truong DM, Long JM, Barshop BA, Kaler G, Nigam SK. Decreased renal organic anion secretion and plasma accumulation of endogenous anions in OAT1 knock-out mice. *J Biol Chem* 281: 5072–5083, 2006.
- Groves CE, Suhre WB, Cherrington NJ, Wright SH. Sex differences in the mRNA, protein, and functional expression of organic anion transporter (Oat) 1, Oat3, and organic cation transporter (Oct) 2 in rabbit renal proximal tubules. *J Pharm Exp Therap* 316: 743–752, 2006.
- Hasegawa M, Kusuhara H, Sugiyama D, Ito K, Ueda S, Endou H, Sugiyama Y. Functional involvement of rat organic anion transporter 3 (rOat3; Slc22a8) in the renal uptake of organic anions. *J Pharm Exp Ther* 300: 746–753, 2002.
- Hosoyamada M, Sekine T, Kanai Y, Endou H. Molecular cloning and functional expression of a multispecific organic anion transporter from human kidney. *Am J Physiol Renal Physiol* 276: F122–F128, 1999.
- Hwang JS, Park EY, Kim WY, Yang CW, Kim J. Expression of OAT1 and OAT3 in differentiating proximal tubules of the mouse kidney. *Histol Histopathol* 25: 33–44, 2010.
- Kikuchi R, Kusuhara H, Sugiyama D, Sugiyama Y. Contribution of organic anion transporter 3 (Slc22a8) to the elimination of p-aminohippuric acid and benzylpenicillin across the blood-brain barrier. *Pharmacol Exp Ther* 306: 51–58, 2003.
- Kobayashi Y, Hirokawa N, Ohshiro N, Sekine T, Sasaki T, Tokuyama S, Endou H, Yamamoto T. Differential gene expression of organic anion transporters in male and female rats. *Biochem Biophys Res Commun* 290: 482–487, 2002.
- Kobayashi Y, Ohshiro N, Tsuchiya A, Kohyama N, Ohbayashi M, Yamamoto T. Renal transport of organic compounds mediated by mouse organic anion transporter 3 (mOAT3). Further substrate specificity of mOAT3. *Drug Metab Dispos* 32: 479–483, 2004.
- Kojima R, Sekine T, Kawachi M, Cha SH, Suzuki Y, Endou H. Immunolocalization of a novel multispecific organic anion transporters, OAT1, OAT2, and OAT3 in rat kidney. *J Am Soc Nephrol* 13: 848–857, 2002.
- Ljubojevic M, Balen D, Breljak D, Kusan M, Anzai N, Bahn A, Burckhardt G, Sabolic I. Renal expression of organic anion transporter OAT2 in rats and mice is regulated by sex hormones. *Am J Physiol Renal Physiol* 292: F361–F372, 2007.
- Ljubojevic M, Herak-Kramberger CM, Hagos Y, Bahn A, Endou H, Burckhardt G, Sabolic I. Rat renal cortical OAT1 and OAT3 exhibit gender differences determined by both androgen stimulation and estrogen inhibition. *Am J Physiol Renal Physiol* 287: F124–F138, 2004.
- Lopez-Nieto CE, You G, Bush KT, Barros EJG, Beier DR, Nigam SK. Molecular cloning and characterization of NKT, a gene product related to the organic cation transporter family that is almost exclusively expressed in the kidney. *J Biol Chem* 272: 6471–6478, 1997.
- Motohashi H, Sakuray Y, Saito H, Masuda S, Urakami Y, Goto M, Fukatsu A, Ogawa O, Inui KI. Gene expression levels and immunolocalization of organic ion transporters in the human kidney. *J Am Soc Nephrol* 13: 866–874, 2002.
- Nagata Y, Kusuhara H, Endou H, Sugiyama Y. Expression and functional characterization of rat organic anion transporter 3 (rOat3) in the choroid plexus. *Mol Pharmacol* 61: 982–988, 2002.
- Nilwarangkoon S, Anzai N, Shiraya K, Yu E, Islam R, Cha SH, Onozato ML, Miura D, Jutabha P, Tojo A, Kanai Y, Endou H. Role of mouse organic anion transporter 3 (mOat3) as a basolateral prostaglandin E2 transport pathway. *J Pharm Sci* 103: 48–55, 2007.
- Ohtsuki S, Kikkawa T, Mori S, Hori S, Takanaga H, Otagiri M, Terasaki T. Mouse reduced in osteosclerosis transporter functions as an organic anion transporter 3 and is localized at abluminal membrane of blood-brain barrier. *J Pharmacol Exp Ther* 309: 1273–1281, 2004.
- Rizwan AN, Burckhardt G. Organic anion transporters of the SLC22 family: biopharmaceutical, physiological, and pathological roles. *Pharm Res* 24: 450–470, 2007.
- Sabolic I, Asif AR, Budach WE, Wanke C, Bahn A, Burckhardt G. Gender differences in kidney function. *Pflügers Arch* 455: 397–429, 2007.
- Sabolic I, Breljak D, Ljubojevic M, Brzica H. Are mice, rats, and rabbits good models for physiological, pharmacological and toxicological studies in humans? *Period Biol* 113: 7–16, 2011.
- Sweet DH. Organic anion transporter (Slc22a) family members as mediators of toxicity. *Toxicol Appl Pharmacol* 204: 198–215, 2005.

34. Sweet DH, Bush KT, Nigam SK. The organic anion transporter family: from physiology to ontogeny and the clinic. *Am J Physiol Renal Physiol* 281: F197–F205, 2001.
35. Sweet DH, Chan LM, Walden R, Yang XP, Miller DS, Pritchard JB. Organic anion transporter 3 (*Slc22a8*) is a dicarboxylate exchanger indirectly coupled to the Na⁺ gradient. *Am J Physiol Renal Physiol* 284: F763–F769, 2003.
36. Sweet DH, Miller DS, Pritchard JB, Fujiwara Y, Beier DR, Nigam SK. Impaired organic anion transport in kidney and choroid plexus of organic anion transporter 3 [*Oat3* (*Slc22a8*)] knockout mice. *J Biol Chem* 277: 26934–26943, 2002.
37. Tojo A, Sekine T, Nakajima N, Hosoyamada M, Kanai Y, Kimura K, Endou H. Immunohistochemical localization of multispecific renal organic anion transporter in rat kidney. *J Am Soc Nephrol* 10: 464–471, 1999.
38. Vallon V, Eraly SA, Rao SR, Gerasimova M, Rose M, Nagle M, Anzai N, Travis S, Sharma K, Nigam SK, Rieg T. A role for the organic anion transporter OAT3 in renal creatinine secretion in mice. *Am J Physiol Renal Physiol* 302: F1293–F1299, 2012.
39. VanWert A, Bailey RM, Sweet DH. Organic anion transporter 3 (*Oat3/Slc22a8*) knockout mice exhibit altered clearance and distribution of penicillin G. *Am J Physiol Renal Physiol* 293: F1332–F1341, 2007.
40. Wright SH, Dantzer WH. Molecular and cellular physiology of renal organic cation and anion transport. *Physiol Rev* 84: 987–1049, 2004.
41. Zhai XY, Birn H, Jensen KB, Thomsen JS, Andreasen A, Christensen E. Digital three-dimensional reconstruction and ultrastructure of the mouse proximal tubule. *J Am Soc Nephrol* 14: 611–619, 2003.

